研究成果の刊行に関する一覧表（服部　信孝）

雑誌

発表者氏名	論文タイトル名	発表誌名	巻号	ページ	出版年
Tomiyama H, Yoshino H, Ogaki K, Li L, Yamashita C, Li Y, Funayama M, Sasaki R, Kokubo Y, Kuzuhara S, Hattori N.	PLA2G6 variant in Parkinson's disease.	J Hum Genet	(in press)	(in press)	2011

研究成果の刊行に関する一覧表（佐藤　栄人）

雑誌

発表者氏名	論文タイトル名	発表誌名	巻号	ページ	出版年
佐藤栄人、服部信孝	Mitochondrial membrane potential decrease caused by loss of PINK1 is not due to proton leak, but to respiratory chain defects.	Neurobiol Dis.	41	118-8	2011

研究成果の刊行に関する一覧表（富山　弘幸）

書籍

著者氏名	論文タイトル名	書籍全体の編集者名	書　籍　名	出版社名	出版地	出版年	ページ
富山弘幸.	遺伝的因子，遺伝学的見地からのパーキンソン病update ―パーキンソン病にどこまで遺伝的要因が関与しているか？―.	山本光利	パーキンソン病（臨床の諸問題2）	中外医学社	東京	2010	37-65.

雑誌

発表者氏名	論文タイトル名	発表誌名	巻号	ページ	出版年
Tomiyama H.	Axon guidance pathway genes and Parkinson's di sease (Commentary).	J Hum Genet.	56	102-3.	2011

研究成果の刊行に関する一覧表（斉木　臣二）

雑誌

発表者氏名	論文タイトル名	発表誌名	巻号	ページ	出版年
Saiki S, Sasazawa Y, Imamichi Y, Kawajiri S, Fujimaki T, Tanida I, Kobayashi H, Sato F, Kei-Ichi Ishikawa, Sato S, Imoto M, Hattori N.	Caffeine induces apoptosis by enhancement of autophagy via PI3K/Akt/mTOR/p70S6K inhibition.	Autophagy	7	176-87	2011
Kawajiri S, Machida Y, Saiki S, Sato S, Hattori N.	Zonisamide reduces cell death in SH-SY5Y cells via an anti-apoptotic effect and by upregulating MnSOD.	Neurosci Lett	481	88-91	2010

研究成果の刊行に関する一覧表（坪井　義夫）

雑誌

発表者氏名	論文タイトル名	発表誌名	巻号	ページ	出版年
坪井義夫、山田達夫	Perry 症候群	MDSJ Letters	3	2-6	2010
坪井義夫	臨床医のための神経病理 Perry 症候群	Clinical Neuroscience	28	366-367	2010
Ohshima S, Tsuboi Y, Yamamoto A, Kawakami M, Farrer MJ, Kira J, Shii H.	Autonomic failures in Perry syndrome with DCTN1 mutation.	Parkinsonism and Related Disorders	16	612-614	2010
坪井義夫	神経情報伝達と疾患 Dynactin 変異と Perry 症候群　モータータンパクと神経変性.	実験医学	28	764-768	2010

研究成果の刊行物・別刷

ARTICLE IN PRESS

YNBDI-02241; No. of pages: 8; 4C:

Neurobiology of Disease xxx (2010) xxx–xxx

Contents lists available at ScienceDirect

Neurobiology of Disease

journal homepage: www.elsevier.com/locate/ynbdi

Mitochondrial membrane potential decrease caused by loss of PINK1 is not due to proton leak, but to respiratory chain defects

Taku Amo [a,1], Shigeto Sato [b], Shinji Saiki [b], Alexander M. Wolf [a], Masaaki Toyomizu [c], Clement A. Gautier [d], Jie Shen [d], Shigeo Ohta [a], Nobutaka Hattori [b,*]

[a] Department of Biochemistry and Cell Biology, Institute of Development and Aging Sciences, Graduate School of Medicine, Nippon Medical School, 1-396 Kosugi-cho, Nakahara-ku, Kawasaki 211-8533, Japan

[b] Department of Neurology, Juntendo University School of Medicine, 2-1-1 Hongo, Bunkyo-ku, Tokyo 113-8421, Japan

[c] Animal Nutrition, Life Sciences, Graduate School of Agricultural Science, Tohoku University, 1-1 Tsutsumidori-Amamiyamachi, Aoba-ku, Sendai 981-8555, Japan

[d] Center for Neurologic Diseases, Brigham and Women's Hospital, Program in Neuroscience, Harvard Medical School, Boston, MA 02115, USA

ARTICLE INFO

Article history:
Received 29 June 2010
Revised 17 August 2010
Accepted 25 August 2010
Available online xxxx

Keywords:
Parkinson's disease
Mitochondria
PINK1
Parkin
Membrane potential
Oxidative phosphorylation
Modular kinetic analysis
Proton leak
Reactive oxygen species

ABSTRACT

Mutations in *PTEN-induced putative kinase 1* (*PINK1*) cause a recessive form of Parkinson's disease (PD). PINK1 is associated with mitochondrial quality control and its partial knock-down induces mitochondrial dysfunction including decreased membrane potential and increased vulnerability against mitochondrial toxins, but the exact function of PINK1 in mitochondria has not been investigated using cells with null expression of PINK1. Here, we show that loss of PINK1 caused mitochondrial dysfunction. In PINK1-deficient ($PINK1^{-/-}$) mouse embryonic fibroblasts (MEFs), mitochondrial membrane potential and cellular ATP levels were decreased compared with those in littermate wild-type MEFs. However, mitochondrial proton leak, which reduces membrane potential in the absence of ATP synthesis, was not altered by loss of PINK1. Instead, activity of the respiratory chain, which produces the membrane potential by oxidizing substrates using oxygen, declined. H_2O_2 production rate by $PINK1^{-/-}$ mitochondria was lower than $PINK1^{+/+}$ mitochondria as a consequence of decreased oxygen consumption rate, while the proportion (H_2O_2 production rate per oxygen consumption rate) was higher. These results suggest that mitochondrial dysfunctions in PD pathogenesis are caused not by proton leak, but by respiratory chain defects.

Introduction

Parkinson's disease (PD) is a neurodegenerative disease characterized by loss of dopaminergic neurons in the substantia nigra. Mitochondrial dysfunction has been proposed as a major factor in the pathogenesis of sporadic and familial PD (Abou-Sleiman et al., 2006). In particular, the identification of mutations in *PTEN-induced putative kinase 1* (*PINK1*) has strongly implicated mitochondrial dysfunction owing to its loss of function in the pathogenesis of PD (Valente et al., 2004). PINK1 contains an N-terminal mitochondrial targeting sequence (MTS) and a serine/threonine kinase domain (Valente et al., 2004). PINK1 kinase activity is crucial for mitochondrial maintenance via TRAP phosphorylation (Pridgeon et al., 2007). Loss of PINK1 function induces increased vulnerability to various stresses (Exner et al., 2007; Haque et al., 2008; Pridgeon et al., 2007; Wood-Kaczmar et al., 2008). However, silencing of PINK1 has only been partial and only one study has been performed to assess mitochondrial functions in steady and artificial states with complete ablation of PINK1 expression (Gautier et al., 2008).

Several studies have shown that PINK1 acts upstream of parkin in the same genetic pathway (Clark et al., 2006; Park et al., 2006) and co-overexpressed PINK1 and parkin both co-localized to mitochondria (Kim et al., 2008). Overexpression of PINK1 promotes mitochondrial fission (Yang et al., 2008). Fission followed by selective fusion segregates dysfunctional mitochondria and permits their removal by autophagy (Twig et al., 2008). PINK1 loss-of-function decreases mitochondrial membrane potential (Chu, 2010) and the PINK1–parkin pathway is associated with mitochondrial elimination in cultured cells treated with the mitochondrial uncoupler carbonyl cyanide *m*-chlorophenylhydrazone (CCCP), which causes mitochondrial depolarization (Geisler et al., 2010; Kawajiri et al., 2010; Matsuda et al., 2010; Narendra et al., 2008, 2010; Vives-Bauza et al., 2010). However, the exact mechanism underlying the mitochondrial depolarization induced by PINK1 defects leading to mitochondrial autophagy has not been examined in detail.

Abbreviations: $\Delta\psi$, mitochondrial membrane potential; FCCP, carbonyl cyanide *p*-trifluoromethoxyphenylhydrazone; MEFs, mouse embryonic fibroblasts; PD, Parkinson's disease; PINK1, PTEN-induced putative kinase 1; ROS, reactive oxygen species; TMRM, tetramethylrhodamine methyl ester; TPMP, triphenylmethylphosphonium.

* Corresponding author. Fax: +81 3 5800 0547.
E-mail address: nhattori@juntendo.ac.jp (N. Hattori).
[1] Present address: Department of Applied Chemistry, National Defense Academy, 1-10-20 Hashirimizu, Yokosuka 239-8686, Japan.

Available online on ScienceDirect (www.sciencedirect.com).

0969-9961/$ – see front matter © 2010 Elsevier Inc. All rights reserved.
doi:10.1016/j.nbd.2010.08.027

Here, we describe a detailed characterization of mitochondria in PINK1-deficient cells. We show that PINK1 deficiency causes a decrease in mitochondrial membrane potential, which is not due to proton leak, but to respiratory chain defects.

Materials and methods

PINK1 knock-out mouse embryonic fibroblasts (MEFs)

PINK1 knock-out MEFs were prepared and cultured as described previously (Matsuda et al., 2010). Mouse embryonic fibroblasts (MEFs) were derived from E12.5 embryos containing littermate 4 mice of each genotype. Embryos were mechanically dispersed by repeated passage through a P1000 pipette tip and plated with MEF media containing DME, 10% FCS, 1× nonessential amino acids, 1 mM L-glutamine, penicillin/streptomycin (invitrogen). The $\psi 2$ cell line, an ecotropic retrovirus packaging cell line, was maintained in Dulbecco's modified Eagle medium (DMEM, Sigma) with 5% fetal bovine serum and 50 μg/ml kanamicin. Transfection of the $\psi 2$ cells with pMESVTS plasmids containing an SV40 large T antigen was performed by lipofection method according to the manual provided by the manufacturer (GIBCO BRL). Five micrograms of the plasmids was used for each transfection. Transfectants were selected by G418 at the concentration of 0.5 mg/ml, and 10 clonal cell lines were established. The highest titer of 5×10^4 cfu/ml was obtained for the conditioned medium of a cell line designated $\psi 2$SVTS1. 10^6 MEFs were plated onto a 10-cm culture dish and kept at 33 °C for 48 hours. Then medium was replaced with 2 ml supplemented with polybrene-supplemented medium conditioned by the $\psi 2$SVTS1 cells at confluency for 3 days. Infection was continued for 3 hours, and the medium was replaced with a fresh one. The infected MEFs were cultured at 33 °C until immortalized cells were obtained.

We confirmed that the differences we detected in this study were due to the PINK1 deficiency, not to artificial effects by immortalization, by measuring cellular respiration rates of not immortalized MEFs from other littermates (Supplemental figure). The respiration rates of not immortalized MEFs were slightly slower than those of immortalized MEFs, but the differences between PINK1$^{+/+}$ and $^{-/-}$ MEFs were consistent (Fig. 2A).

Cell growth

Cells were seeded in 12-well plates at density of $3\sim6 \times 10^3$ cells/well and incubated in DMEM high glucose medium (4.5 g/l glucose and 1 mM sodium pyruvate) supplemented with 10% fetal bovine serum. After a day, the medium was replaced with DMEM glucose-free medium supplemented with 1 g/l galactose, 1 mM sodium pyruvate and 10% fetal bovine serum (DMEM galactose medium) at 37 °C in an incubator with a humidified atmosphere of 5% CO_2. Cells were trypsinized and live cells were assessed by trypan blue dye exclusion.

Mitochondrial morphological changes

Cells were seeded in 6-well plates at 2.0×10^5/well and incubated in DMEM high glucose medium (4.5 g/l glucose and 1 mM sodium pyruvate) supplemented with 10% fetal bovine serum and 1% penicillin/streptomycin. After a day, the medium was replaced with DMEM glucose-free medium supplemented with 1 g/l galactose, 1 mM sodium pyruvate and 10% fetal bovine serum (DMEM galactose medium) at 37 °C in an incubator with a humidified atmosphere of 5% CO_2. 24 hours later, cells were fixed and immunostained with anti-Tom20 antibody to visualize mitochondria according to a protocol as previously described (Kawajiri et al., 2010). All images were obtained using an Axioplan 2 imaging microscope (Carl Zeiss, Oberkochen, Germany).

Cellular ATP levels

Intracellular ATP levels were determined by a cellular ATP assay kit (TOYO B-Net, Tokyo, Japan) according to the manufacturer's instructions using a Lumat LB9507 luminometer (Berthold Technology, Bad Wildbad, Germany).

Membrane potential

Fluorescence images were recorded using a multi-dimensional imaging workstation (AS MDW, Leica Microsystems, Wetzlar, Germany) with a climate chamber maintained at 37 °C. Fluorescence was quantified with a CCD camera (CoolSnap HQ, Roper Scientific, Princeton, NJ) using a 20× objective. Cells were stained for 1 hour with a non-quenching concentration (20 nM) of tetramethylrhodamine methyl ester (TMRM) in a 96-well plate. The cell-permeable cationic dye TMRM accumulates in mitochondria according to the Nernst equation. Nuclei were stained with 250 nM Hoechst 34580. Mitochondrial TMRM fluorescence was integrated in a 40-μm diameter circular area around the nucleus, and the minimum fluorescence in this area was subtracted as background fluorescence.

Cell respiration

Cell respiration was measured at 37 °C using the Oxygen Meter Model 781 and the Mitocell MT200 closed respiratory chamber (Strathkelvin Instruments, North Lanarkshire, United Kingdom). Cells were cultured in DMEM with 4.5 g/l of glucose supplemented with 10% FBS. Cells were then trypsinized and resuspended in Leibovitz's L-15 medium (Invitrogen) at density of 8.0×10^6 cells/ml. The oxygen respiration rate was measured under each of the following three conditions: basal rate (no additions); State 4 (no ATP synthesis) [after addition of 1 μg/ml oligomycin (Sigma)], uncoupled [after addition of 3 μM FCCP (carbonyl cyanide *p*-trifluoromethoxyphenylhydrazone; Sigma)] using Strathkelvin 949 Oxygen System. After sequential measurements, the endogenous respiration rate was determined by adding 1 μM rotenone + 2 μM myxothiazol.

Mitochondrial respiration and membrane potential

Mitochondria were prepared from cultured MEFs as previously described (Amo and Brand, 2007). Mitochondrial oxygen consumption with 5 mM succinate as a respiratory substrate was measured at 37 °C using a Clark electrode (Rank Brothers, Cambridge, United Kingdom) calibrated with air-saturated respiration buffer comprising 0.115 M KCl, 10 mM KH_2PO_4, 3 mM HEPES (pH 7.2), 2 mM $MgCl_2$, 1 mM EGTA and 0.3% (w/v) defatted BSA, assumed to contain 406 nmol atomic oxygen/ml (Reynafarje et al., 1985). Mitochondrial membrane potential ($\Delta\psi$) was measured simultaneously with respiratory activity using an electrode sensitive to the lipophilic cation $TPMP^+$ (triphenylmethylphosphonium) (Brand, 1995). Mitochondria were incubated at 0.5 mg/ml in the presence of 80 ng/ml nigericin (to collapse the pH gradient so that the proton motive force was expressed exclusively as $\Delta\psi$) and 2 μM rotenone (to inhibit complex I). The $TPMP^+$-sensitive electrode was calibrated with sequential additions of $TPMP^+$ up to 2 μM, then 5 mM succinate was added to initiate respiration. Experiments were terminated with 2 μM FCCP, allowing correction for any small baseline drift. $\Delta\psi$ was calculated from the distribution of $TPMP^+$ across the mitochondrial inner membrane using a binding correction factor of 0.35 mg protein/μl. Respiratory rates with 4 mM pyruvate + 1 mM malate as a substrate in State 3 (with 0.25 mM ADP) and State 4 (with 1 μg/ml oligomycin) were determined using the Oxygen Meter Model 781 and the Mitocell MT200 closed respiratory chamber (Strathkelvin Instruments).

Please cite this article as: Amo, T., et al., Mitochondrial membrane potential decrease caused by loss of PINK1 is not due to proton leak, but to respiratory chain defects, Neurobiol. Dis. (2010), doi:10.1016/j.nbd.2010.08.027

Modular kinetic analysis

To investigate differences in oxidative phosphorylation caused by PINK1 knock-out, we applied a systems approach, namely modular kinetic analysis (Amo and Brand, 2007; Brand, 1990). This analyzes the kinetics of the whole of oxidative phosphorylation divided into three modules connected by their common substrate or product, $\Delta\psi$. The modules are (i) the reactions that produce $\Delta\psi$, consisting of the substrate translocases, dehydrogenases and other enzymes and the components of the respiratory chain, called 'substrate oxidation'; (ii) the reactions that consume $\Delta\psi$ and synthesize, export and dephosphorylate ATP, consisting of ATP synthase, the phosphate and adenine nucleotide translocases and any ATPases that may be present, called the 'phosphorylating system'; and (iii) the reactions that consume $\Delta\psi$ without ATP synthesis, called the 'proton leak' (Brand, 1990). The analysis reports changes anywhere within oxidative phosphorylation that are functionally important but is unresponsive to changes that have no functional consequences. Comparison of the kinetic responses of each of the three modules to $\Delta\psi$ obtained using mitochondria isolated from PINK1$^{+/+}$ and PINK1$^{-/-}$ MEFs would reveal any effects of PINK1 on the kinetics of oxidative phosphorylation. Oxygen consumption and $\Delta\psi$ were measured simultaneously using mitochondria incubated with 80 ng/ml nigericin and 4 μM rotenone. Respiration was initiated by 5 mM succinate. The kinetic behavior of a '$\Delta\psi$-producer' can be established by specific modulation of a $\Delta\psi$-consumer and the kinetics of a consumer can be established by specific modulation of a $\Delta\psi$-producer (Brand, 1998). To measure the kinetic response of proton leak to $\Delta\psi$, the State 4 (non-phosphorylating) respiration of mitochondria in the presence of oligomycin (0.8 μg/ml; to prevent any residual ATP synthesis), which was used solely to drive the proton leak, was titrated with malonate (up to 8 mM). In a similar way, State 4 respiration was titrated by FCCP (up to 1 μM) for measurement of the kinetic response of substrate oxidation to $\Delta\psi$. State 3 (maximal rate of ATP synthesis) was obtained by addition of excess ADP (1 mM). Titration of State 3 respiration with malonate (up to 1.1 mM) allowed measurement of the kinetics of the $\Delta\psi$-consumers (the sum of the phosphorylating system and proton leak). The coupling efficiencies of oxidative phosphorylation were calculated from the kinetic curves as the percentage of mitochondrial respiration rate at a given $\Delta\psi$ that was used for ATP synthesis and was therefore inhibited by oligomycin. Note that any slip reactions will appear as proton leak in this analysis (Brand et al., 1994).

Mitochondrial ROS production

Mitochondrial ROS production rate was assessed by measurement of H_2O_2 generation rate, determined fluorometrically by measurement of oxidation of Amplex Red to fluorescent resorufin coupled to the enzymatic reduction of H_2O_2 by horseradish peroxidase using a spectrofluorometer RF-5300PC (Shimadzu, Kyoto, Japan). The H_2O_2 generation rate was measured in non-phosphorylating conditions (=State 4) using either pyruvate/malate or succinate as respiratory substrates. Mitochondria were incubated at 0.1 mg/ml in respiration buffer. All incubations also contained 5 μM Amplex Red, 2 U/ml horseradish peroxidase and 8 U/ml superoxide dismutase. The reaction was initiated by addition of 5 mM succinate or 4 mM pyruvate + 1 mM malonate and the increase in fluorescence was followed at excitation and emission wavelengths of 560 and 590 nm, respectively. Appropriate correction for background signals and standard curves generated using known amounts of H_2O_2 were used to calculate the rate of H_2O_2 production in nmol/min/mg mitochondrial protein. The percentage free radical leak, which is a measure of the number of electrons that produce superoxide (and subsequently H_2O_2) compared with the total number of electrons which pass thorough the respiratory chain, was calculated as the rate of H_2O_2 production divided by the rate of O_2 consumption (Barja et al., 1994).

Statistics

Values are presented as means ± SEM except Fig. 2D, in which error bars indicate SD. The significance of differences between means was assessed by the unpaired Student's *t*-test using Microsoft Excel; *P* values <0.05 were taken to be significant.

Results

Cell growth and mitochondrial morphology

In general, cultured cells gain their energy mostly from glycolysis. Therefore, cells deficient in respiratory function can grow in normal medium, although possibly at a slower rate, relying predominantly on glycolysis (Hofhaus et al., 1996). Actually, ρ^0 cells, which lack mitochondrial DNA completely, can grow producing energy exclusively through glycolysis (King and Attardi, 1989). On the other hand, galactose metabolism via glycolysis is much slower than glucose metabolism (Reitzer et al., 1979). Therefore, cells in galactose medium are forced to oxidize pyruvate through the mitochondrial respiratory chain for energy required for growth. Consequently, cells with defects in their mitochondrial respiratory chains show growth impairments in galactose medium. To evaluate this phenomenon is also observed in our cells, we examined growth retardation by addition of mitochondrial complex I inhibitor, rotenone (Fig. 1A). In glucose medium, 10 nM rotenone had only a slight effect on the growth of PINK1$^{+/+}$ MEFs and slower growth was observed even in the presence of 100 nM rotenone. However, in the galactose medium, 10 nM rotenone significantly inhibited the growth of PINK1$^{+/+}$ MEFs and 100 nM roteone completely arrested the growth. Therefore, we could confirm that the growth impairment of our cells in the galactose medium was due to mitochondrial respiratory chain defects.

PINK1 acts upstream of parkin, regulating mitochondrial integrity and function; therefore, loss of PINK1 is considered to affect mitochondrial functions. To assess the mitochondrial functions of PINK1$^{-/-}$ MEFs, growth capability in a medium in which galactose replaced glucose was examined. As shown in Fig. 1B, PINK1$^{-/-}$ MEFs appeared to show clear growth impairments in the galactose medium, whereas PINK1$^{+/+}$ MEFs grew slightly slower than in the glucose medium.

No differences of mitochondrial morphology between PINK1$^{+/+}$ and $^{-/-}$ MEFs in the glucose medium were detected (Fig. 1C), consistent with the previous report (Matsuda et al., 2010). However, in the galactose medium, mitochondria of the PINK1$^{-/-}$ MEFs were more fragmented compared to the PINK$^{+/+}$ MEFs (Fig. 1C). This is consistent with previous reports, which found mitochondrial morphological changes were more pronounced when PINK1 knock-down HeLa cells were grown in low-glucose medium (Exner et al., 2007) and human PINK1 homozygous mutant fibroblast in galactose medium (Grünewald et al., 2009). In these cells, mitochondrial morphological changes were associated with the mitochondrial functional impairment.

Assessments of mitochondrial functions at the cellular level

Because PINK1$^{-/-}$ MEFs showed severe growth impairments in the galactose medium, the mitochondrial functions of these cells were assessed at the cellular level. First, cellular respiration rates were measured (Fig. 2A). The basal respiration rate was significantly reduced in PINK1$^{-/-}$ cells compared with that in PINK1$^{+/+}$ cells (11.13 ± 0.71 versus 14.36 ± 1.01 nmol O/min/10^6 cells; $p<0.05$; $n=5$ independent experiments), consistent with previous reports using partial knock-down of PINK1 expression (Gandhi et al., 2009; Liu et al., 2009). Oligomycin inhibits ATP synthase, resulting in non-phosphorylating respiration. FCCP uncouples oxidative phosphorylation, leading to maximum respiration rates. In both conditions, the

Please cite this article as: Amo, T., et al., Mitochondrial membrane potential decrease caused by loss of PINK1 is not due to proton leak, but to respiratory chain defects, Neurobiol. Dis. (2010), doi:10.1016/j.nbd.2010.08.027

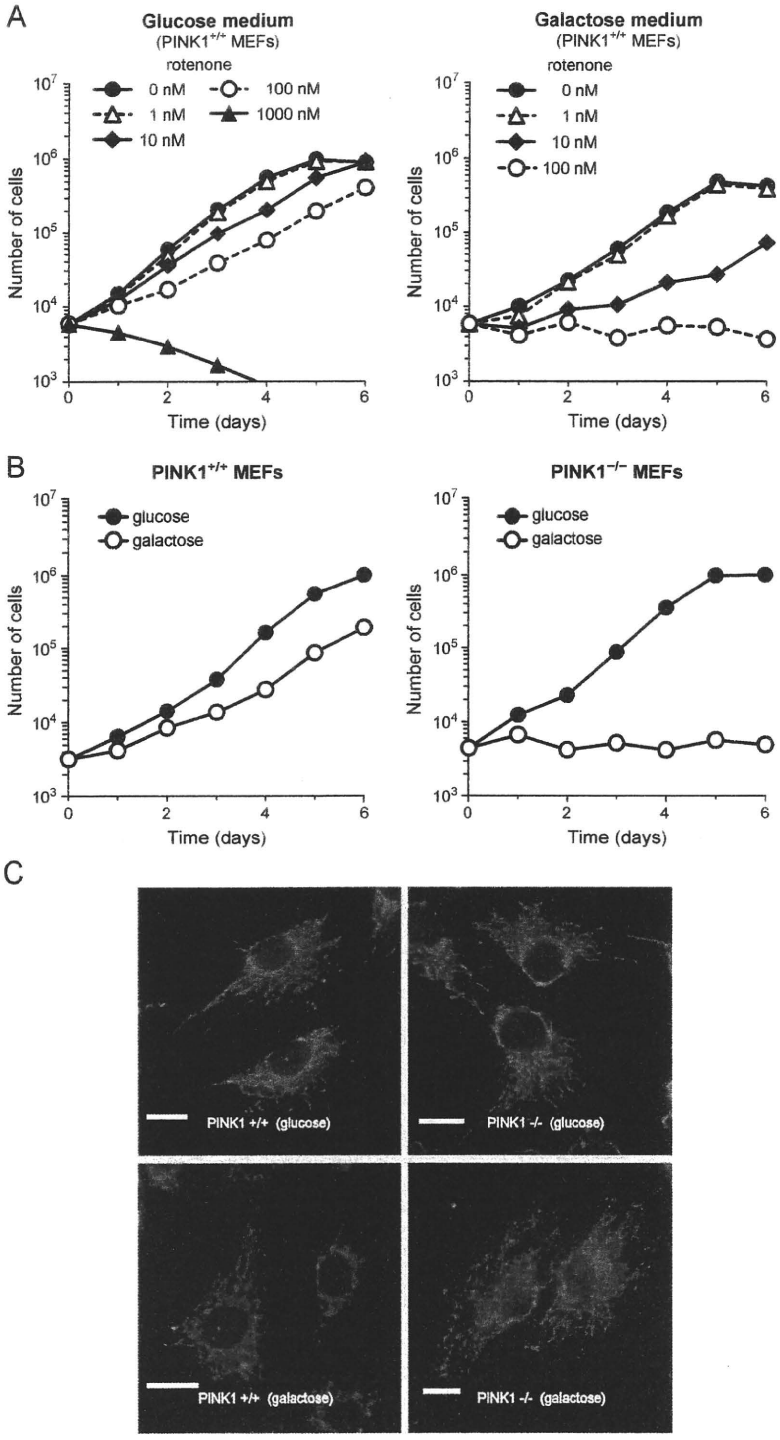

Fig. 1. (A) Growth retardation of PINK1$^{+/+}$ MEFs by mitochondrial complex I inhibitor, rotenone in glucose or galactose medium. Closed circles with solid line, 0 nM rotenone; open triangles with dashed line, 1 nM rotenone; closed diamonds with solid line, 10 nM rotenone; open circles with dashed line, 100 nM rotenone; closed triangles with solid line, 1000 nM rotenone. Cells grown in 12-well plates were trypsinized and live cells were assessed by trypan blue dye exclusion. (B) Growth curves of PINK1$^{+/+}$ and $^{-/-}$ MEFs. Closed symbols (*glucose*), growth curve for cells grown in DMEM containing 4.5 g/l glucose and 1 mM sodium pyruvate; open symbols (*galactose*), growth curve for cells grown in DMEM lacking glucose and containing instead 1.0 g/l galactose and 1 mM sodium pyruvate. Cells grown in 12-well plates were trypsinized and live cells were assessed by trypan blue dye exclusion. (C) Mitochondrial morphology of PINK1$^{+/+}$ and $^{-/-}$ MEFs. After incubating cells with the glucose or galactose medium for 24 hours, cells were fixed and immunostained with anti-Tom20 antibody to visualize mitochondria. Scale bar, 20 μm.

PINK1$^{-/-}$ cells respired significantly slower than the PINK1$^{+/+}$ cells (1.76 ± 0.13 versus 2.95 ± 0.27 ($p<0.01$; $n=5$ independent experiments) and 16.44 ± 1.80 versus 23.50 ± 1.18 nmol O/min/10^6 cells ($p<0.05$; $n=5$ independent experiments), respectively).

The main function of mitochondria is ATP synthesis via oxidative phosphorylation. ATP levels under basal conditions were significantly reduced in PINK1$^{-/-}$ MEFs (Fig. 2B), as reported previously for dissociated PINK1$^{-/-}$ mouse neurons (Gispert et al., 2009) and PINK1

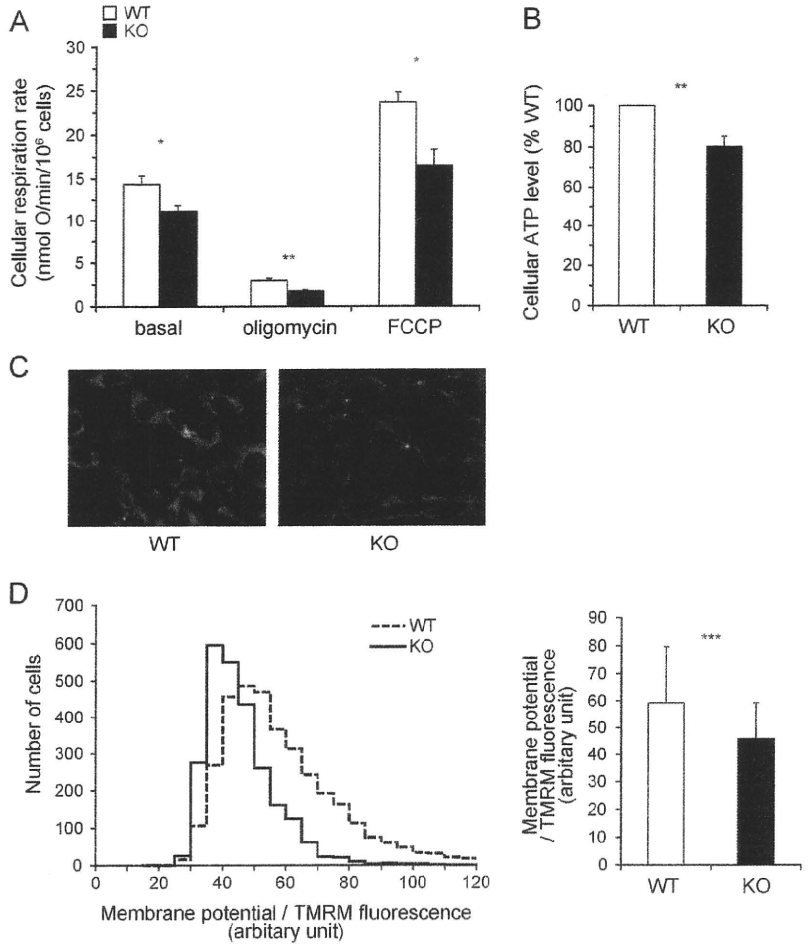

Fig. 2. Mitochondrial functions assessed at the cellular level. Open bars, PINK1$^{+/+}$ MEFs; closed bars, PINK1$^{-/-}$ MEFs. (A) Cell respiration rate of PINK1$^{+/+}$ and $^{-/-}$ MEFs. The oxygen respiration rate was measured at density of 8.0×10^6 cells/ml under each of the following three conditions: basal rate (no additions); State 4 (no ATP synthesis) [after addition of 1 μg/ml oligomycin], uncoupled [after addition of 3 μM FCCP]. After sequential measurements, the endogenous respiration rate was determined by adding 1 μM rotenone +2 μM myxothiazol. Error bars indicate SEM ($n=5$ independent experiments). (B) Cellular ATP levels. Data were normalized based on cell numbers and expressed as the percentage of the level in PINK1$^{+/+}$ cells. Error bars indicate SEM ($n=4$ independent experiments). (C) Live cell images of PINK1$^{+/+}$ and $^{-/-}$ MEFs with TMRM fluorescence. (D) Mitochondrial membrane potential evaluated by live cell imaging of TMRM fluorescence. *Left panel*, the distribution of TMRM fluorescence from 3537 PIINK1$^{+/+}$ and 2566 PINK1$^{-/-}$ cells from 12 wells per cell type; *right panel*, the average value of TMRM fluorescence per cell. Error bars indicate SD. *$P<0.05$; **$P<0.01$; ***$P<0.001$.

siRNA knock-down PC12 cells (Liu et al., 2009). Mitochondrial membrane potential was also measured by live cell imaging of TMRM fluorescence. Typical images were shown in Fig. 2C. The histogram shows the distribution of TMRM fluorescence from 3537 PINK1$^{+/+}$ cells and 2566 PINK1$^{-/-}$ cells from 12 wells per cell type and the bar graph indicates the mean ± SD of TMRM fluorescence per cell (Fig. 2D). According to the Nernst equation, the ratio of TMRM fluorescence would translate into, on average, 6.88 mV lower mitochondrial membrane potential in the PINK1$^{-/-}$ cells if the plasma membrane potentials were not different between PINK1$^{+/+}$ and $^{-/-}$ cells. Mitochondrial membrane potential decrease was also showed previously in PINK1 knock-down HeLa cells (Exner et al., 2007) and in stable PINK1 knock-down neuroblastoma cell lines (Sandebring et al., 2009).

Assessments of mitochondrial functions using isolated mitochondria

To further analyze mitochondrial functions, we measured the kinetics of oxidative phosphorylation using isolated mitochondria from PINK1$^{+/+}$ and $^{-/-}$ MEFs. Fig. 3 shows the kinetics of the three modules of oxidative phosphorylation using succinate as a respiratory substrate (complex II-linked respiration). Fig. 3A shows the kinetic response of substrate oxidation to its product, $\Delta\psi$. The substrate oxidation kinetic curve for PINK1$^{-/-}$ cells was clearly shifted lower compared with that for PINK1$^{+/+}$ cells, indicating that the loss of PINK1 caused mitochondrial respiratory chain defects. Fig. 3B shows the kinetic response of proton leak to its driving force, $\Delta\psi$, and Fig. 3C shows the kinetic response of the ATP phosphorylating pathway to its driving force, $\Delta\psi$. Both kinetic curves for PINK1$^{+/+}$ and $^{-/-}$ MEFs (open and closed symbols, respectively) were overlapping, implying that there were no significant differences in those modules.

We also independently measured the mitochondrial oxygen consumption rate using pyruvate/malate as a respiratory substrate instead of succinate to check complex I. Modular kinetic analysis using pyruvate/malate is technically difficult for the following reasons: (1) the oxygen consumption rate with pyruvate/malate is much slower than succinate respiration; and (2) there are no competitive inhibitors of complex I-linked respiration, such as malonate for succinate respiration. As shown in Fig. 4A, the respiration rates in State 3 and 4 with pyruvate/malate of isolated mitochondria from PINK1$^{-/-}$ cells (closed symbols) were significantly slower than those of PINK1$^{+/+}$ cells (open symbols), as in the case of succinate respiration (Fig. 4B; data derived from the kinetic curves in Fig. 3).

Please cite this article as: Amo, T., et al., Mitochondrial membrane potential decrease caused by loss of PINK1 is not due to proton leak, but to respiratory chain defects, Neurobiol. Dis. (2010), doi:10.1016/j.nbd.2010.08.027

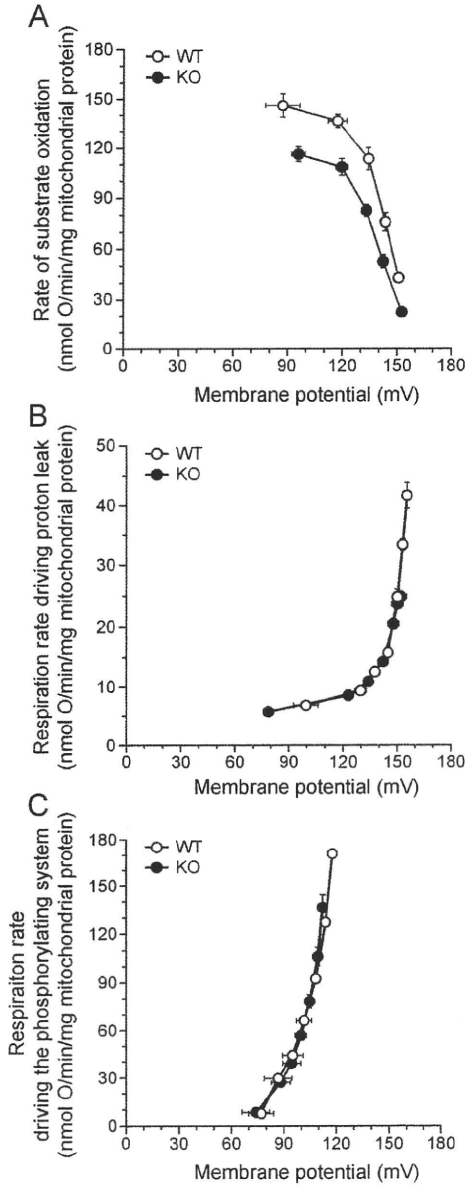

Fig. 3. Modular kinetic analysis of oxidative phosphorylation in mitochondria isolated from PINK1$^{+/+}$ and $^{-/-}$ MEFs. Modular kinetic analysis of the kinetic responses to membrane potential, $\Delta\psi$, of respiration driving (A) substrate oxidation ($\Delta\psi$ titrated with uncoupler, FCCP, starting in State 4), (B) proton leak ($\Delta\psi$ titrated with malonate, starting in State 4) and (C) the phosphorylating system, calculated by subtracting respiration driving proton leak from respiration driving the $\Delta\psi$-consumers ($\Delta\psi$ titrated with malonate starting in State 3; not shown) at each $\Delta\psi$. Open symbols, PINK1$^{+/+}$ MEFs; closed symbols, PINK1$^{-/-}$ MEFs. Error bars indicate SEM ($n=4$ independent mitochondrial preparations).

Mitochondrial ROS production

Mitochondrial ROS production rate was assessed by measurement of the H_2O_2 generation rate. Mechanisms of mitochondrial ROS production were well described elsewhere (Fig. 1 of Lambert et al., 2010). Pyruvate and malate generate NADH, which induced forward electron transport and generate ROS mainly from complex I and III. For pyruvate/malate respiration, the basal H_2O_2 generation rate (measured in the absence of respiratory chain inhibitors) was not different between PINK1$^{+/+}$ and $^{-/-}$ mitochondria (Fig. 4C). The addition of antimycin A and further addition of rotenone, which inhibited forward electron transport at complex III and I, respectively, enhanced H_2O_2 generation. During succinate respiration in the absence of respiratory chain inhibitors, ROS are generated mainly from the quinine binding site of complex I due to reverse electron flow from coenzyme Q to complex I. For succinate respiration, H_2O_2 generation rate in the absence of reparatory chain inhibitors was higher in PINK1$^{+/+}$ mitochondria than in PINK1$^{-/-}$ mitochondria, but the difference was not significant (Fig. 4D). The addition of rotenone, which blocks reverse electron flow from coenzyme Q to complex I, attenuated H_2O_2 generation.

Figs. 4 C and D show a tendency for PINK1$^{+/+}$ mitochondria to generate more ROS than PINK1$^{-/-}$ mitochondria. However, their respiration rates were remarkably different (Figs. 4A and B). Therefore, we calculated the percentage free radical leak, which is the fraction of molecules of O_2 consumed that give rise to H_2O_2 release by mitochondria (free radical leak) during either pyruvate/malate or succinate State 4 respiration (Figs. 4E and F). For pyruvate/malate respiration, mitochondria isolated from PINK1$^{-/-}$ cells had higher proportion of H_2O_2 generation than PINK1$^{+/+}$ mitochondria. During succinate respiration without respiratory inhibitors, PINK1$^{-/-}$ mitochondria had also higher proportion of free radical leak mainly from complex I due to reverse electron flow from coenzyme Q to complex I. Because the differences disappeared with addition of rotenone, which inhibit reverse electron flow, ROS generation enhanced by loss of PINK1 was mostly from complex I.

Discussion

We produced an *in vitro* model of Parkinson's disease, immortalized PINK1$^{-/-}$ MEFs. Previously, impairment of mitochondrial respiration was observed in the brains of PINK1$^{-/-}$ mice (Gautier et al., 2008). PINK1$^{-/-}$ MEFs clearly showed a phenotype of mitochondrial dysfunctions, which is consistent with PD pathogenesis. This phenotype was apparent in a cell growth experiment using medium containing galactose instead of glucose (Fig. 1B). Mitochondrial fragmentation was observed when PINK1$^{-/-}$ MEFs grew in the galactose medium (Fig. 1C), which was consistent with previous reports (Exner et al., 2007; Grünewald et al., 2009). Our results have unveiled that the PINK1$^{-/-}$ MEF line could be a potential PD model, presenting growth retardation due to decreased mitochondrial respiration activity. Thus, the PINK1$^{-/-}$ MEFs are a useful tool for evaluating the role of PINK1 in mitochondrial dysfunction and relevant to PD.

In PINK1$^{-/-}$ MEFs, mitochondrial membrane potential was decreased compared with that in littermate wild-type MEFs (Figs. 2C and D), as reported previously for PINK1 knock-down HeLa cells (Exner et al., 2007) and stable PINK1 knock-down neuroblastoma cell lines (Sandebring et al., 2009). This is a key event during elimination of mitochondria. Mitochondrial fission followed by selective fusion segregates damaged mitochondria, which decreases their membrane potential, and permits their removal by autophagy (Twig et al., 2008). The PINK1–parkin pathway is thought to have a crucial role in this mitochondrial elimination mechanism (Geisler et al., 2010; Kawajiri et al., 2010; Matsuda et al., 2010; Narendra et al., 2008, 2010; Vives-Bauza et al., 2010). To clarify what caused the decrease in mitochondrial membrane potential, we performed a modular kinetic analysis using isolated mitochondria (Fig. 3). This analyzes the kinetics of the whole of oxidative phosphorylation divided into three modules connected by their common substrate or product, mitochondrial membrane potential ($\Delta\psi$). The modules are include one $\Delta\psi$-producer (substrate oxidation) and two $\Delta\psi$-consumers (phosphorylating system and proton leak) (Brand, 1990). To decrease $\Delta\psi$, the $\Delta\psi$-producer should be down-regulated and/or $\Delta\psi$-consumers should be up-regulated. As cellular ATP levels were decreased compared with those in littermate wild-type MEFs (Fig. 2B), it is unlikely that the phosphorylating system is up-regulated. Indeed, the kinetics of the phosphorylation module were not altered (Fig. 3C). The other $\Delta\psi$-consumer, proton leak,

Please cite this article as: Amo, T., et al., Mitochondrial membrane potential decrease caused by loss of PINK1 is not due to proton leak, but to respiratory chain defects, Neurobiol. Dis. (2010), doi:10.1016/j.nbd.2010.08.027

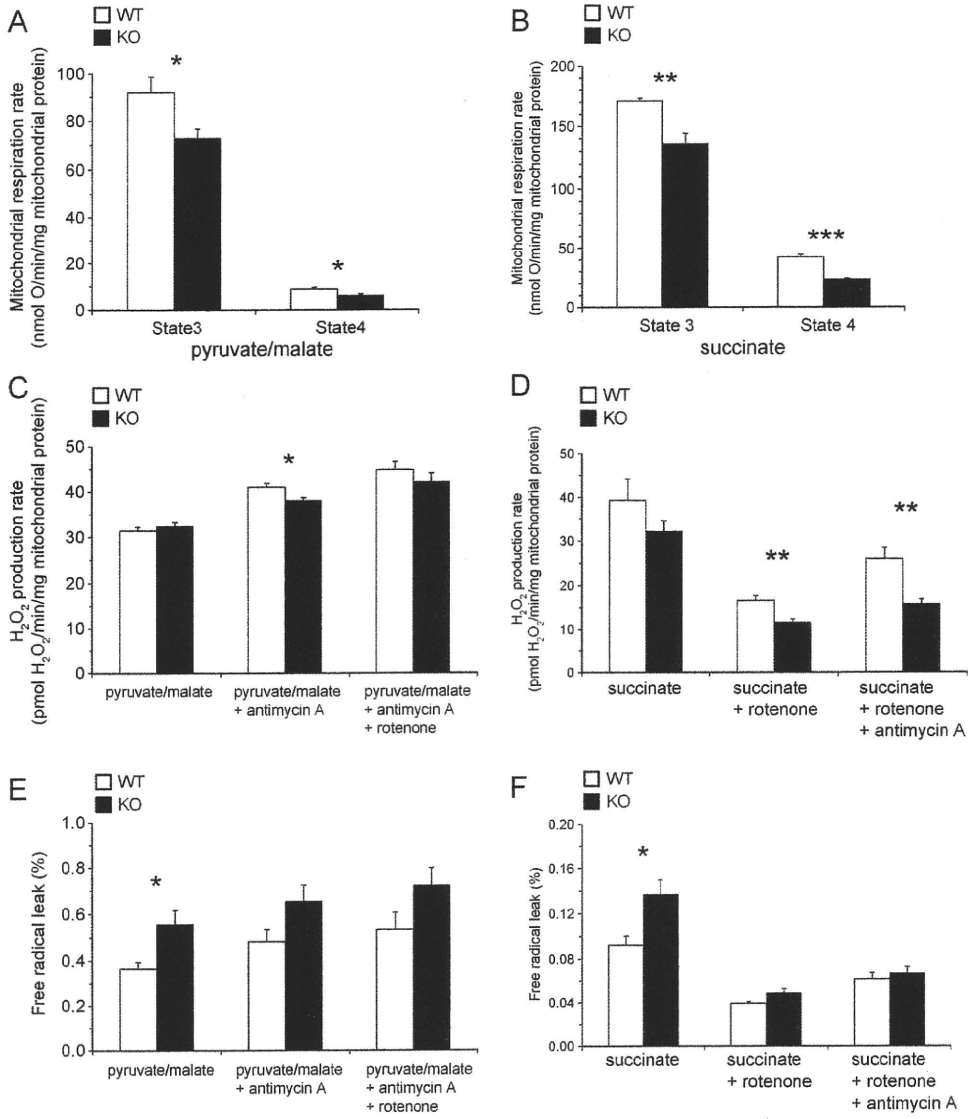

Fig. 4. Oxygen consumption rate and H_2O_2 production rate of mitochondria isolated from PINK1$^{+/+}$ and $^{-/-}$ MEFs. Open bars, PINK1$^{+/+}$ MEFs; closed bars, PINK1$^{-/-}$ MEFs. (A) State 3 and State 4 respiration rate of mitochondria with pyruvate/malate as a respiratory substrate. (B) State 3 and State 4 respiration rate of mitochondria with succinate as a respiratory substrate. Data were derived from the results of modular kinetic analysis (Fig. 3). State 3 respiration rates were the kinetic start points of the $\Delta\psi$-consumers (the sum of the phosphorylating system and proton leak). State 4 respiration rates were average values of the respiration rates at the kinetic start points of substrate oxidation and proton leak. (C, D) Mitochondrial H_2O_2 production rate with pyruvate/malate (C) or succinate (D) as a respiratory substrate. (E, F) Percentage free radical leak (FRL) for State 4 respiration with pyruvate/malate (E) or succinate (F) as a respiratory substrate. Error bars indicate SEM ($n=5$ and 4 independent mitochondrial preparations for pyruvate/malate and succinate respiration, respectively). *$P<0.05$; **$P<0.01$; ***$P<0.001$.

which partially dissipates the membrane potential without ATP synthesis, was also not changed (Fig. 3B). Therefore, the decrease in membrane potential caused by loss of PINK1 is likely to have been caused only by lower activity of the $\Delta\psi$-producer, substrate oxidation (Fig. 3A). This is the first report showing that mitochondrial membrane potential decrease caused by loss of PINK1, which is the key event for the following mitochondrial elimination, was not due to proton leak, but to respiratory chain defects. We used only succinate (a complex II-linked substrate) as a respiratory substrate in the modular kinetic analysis for technical reasons. However, complex I-linked respiration (pyruvate/malate) was also decreased in PINK1$^{-/-}$ MEFs like succinate respiration (Fig. 4A).

The mitochondrial respiration rates in State 4 were decreased in PINK1$^{-/-}$ MEFs, and consequently, the proportions of free radical leak were significantly higher in PINK1$^{-/-}$ MEFs than in PINK1$^{+/+}$ MEFs (Figs. 4E and F). Because the differences disappeared with addition of rotenone (complex I inhibitor, which inhibits reverse electron flow from coenzyme Q to complex I), ROS generation enhanced by loss of PINK1 was mostly from complex I. These results are partially consistent with those in previous reports, suggesting that MPTP and rotenone induce neuronal cell death by inhibiting complex I activity, leading to a PD-like phenotype (Dauer and Przedborski, 2003; Jackson-Lewis and Przedborski, 2007; Trojanowski, 2003).

In this study, we developed an *in vitro* PD model, the PINK1$^{-/-}$ MEF line, and established the experimental conditions for cell growth to detect mitochondrial dysfunction. This is the first report showing that complete ablation of PINK1 causes a decrease in mitochondrial membrane potential, which is not due to proton leak, but to respiratory chain defects.

Please cite this article as: Amo, T., et al., Mitochondrial membrane potential decrease caused by loss of PINK1 is not due to proton leak, but to respiratory chain defects, Neurobiol. Dis. (2010), doi:10.1016/j.nbd.2010.08.027

Supplementary materials related to this article can be found online at doi:10.1016/j.nbd.2010.08.027.

Acknowledgements

This work was supported by a Grant-in-Aid for Scientific Research for Young Scientists (B) from JSPS (T.A. and S.Saiki), a JSPS fellowship (T.A.), Nagao Memorial Fund (S. Saiki) and a Grant from Takeda Scientific Foundation (S. Saiki and T.A.). We thank Dr. Noriyuki Matsuda for assistance to obtain immortalized cells.

References

Abou-Sleiman, P.M., Muqit, M.M., Wood, N.W., 2006. Expanding insights of mitochondrial dysfunction in Parkinson's disease. Nat. Rev. Neurosci. 7, 207–219.

Amo, T., Brand, M.D., 2007. Were inefficient mitochondrial haplogroups selected during migrations of modern humans? A test using modular kinetic analysis of coupling in mitochondria from cybrid cell lines. Biochem. J. 404, 345–351.

Barja, G., Cadenas, S., Rojas, C., Pérez-Campo, R., López-Torres, M., 1994. Low mitochondrial free radical production per unit O_2 consumption can explain the simultaneous presence of high longevity and high aerobic metabolic rate in birds. Free Radic. Res. 21, 317–327.

Brand, M.D., 1990. The proton leak across the mitochondrial inner membrane. Biochim. Biophys. Acta 1018, 128–133.

Brand, M.D., 1995. Measurement of mitochondrial protonmotive force. In: Brown, G.C., Cooper, C.E. (Eds.), Bioenergetics, a practical approach. IRL Press, Oxford, pp. 39–62.

Brand, M.D., 1998. Top-down elasticity analysis and its application to energy metabolism in isolated mitochondria and intact cells. Mol. Cell. Biochem. 184, 13–20.

Brand, M.D., Chien, L.F., Diolez, P., 1994. Experimental discrimination between proton leak and redox slip during mitochondrial electron transport. Biochem. J. 297, 27–29.

Chu, C.T., 2010. Tickled PINK1: mitochondrial homeostasis and autophagy in recessive Parkinsonism. Biochim. Biophys. Acta 1802, 20–28.

Clark, I.E., Dodson, M.W., Jiang, C., Cao, J.H., Huh, J.R., Seol, J.H., Yoo, S.J., Hay, B.A., Guo, M., 2006. *Drosophila pink1* is required for mitochondrial function and interacts genetically with *parkin*. Nature 441, 1162–1166.

Dauer, W., Przedborski, S., 2003. Parkinson's disease: mechanisms and models. Neuron 39, 889–909.

Exner, N., Treske, B., Paquet, D., Holmstrom, K., Schiesling, C., Gispert, S., Carballo-Carbajal, I., Berg, D., Hoepken, H.H., Gasser, T., Krüger, R., Winklhofer, K.F., Vogel, F., Reichert, A.S., Auburger, G., Kahle, P.J., Schmid, B., Haass, C., 2007. Loss-of-function of human PINK1 results in mitochondrial pathology and can be rescued by parkin. J. Neurosci. 27, 12413–12418.

Gandhi, S., Wood-Kaczmar, A., Yao, Z., Plun-Favreau, H., Deas, E., Klupsch, K., Downward, J., Latchman, D.S., Tabrizi, S.J., Wood, N.W., Duchen, M.R., Abramov, A.Y., 2009. PINK1-associated Parkinson's disease is caused by neuronal vulnerability to calcium-induced cell death. Mol. Cell 33, 627–638.

Gautier, C.A., Kitada, T., Shen, J., 2008. Loss of PINK1 causes mitochondrial functional defects and increased sensitivity to oxidative stress. Proc. Natl. Acad. Sci. U. S. A. 105, 11364–11369.

Geisler, S., Holmström, K.M., Skujat, D., Fiesel, F.C., Rothfuss, O.C., Kahle, P.J., Springer, W., 2010. PINK1/Parkin-mediated mitophagy is dependent on VDAC1 and p62/SQSTM1. Nat. Cell Biol. 12, 119–131.

Gispert, S., Ricciardi, F., Kurz, A., Azizov, M., Hoepken, H.H., Becker, D., Voos, W., Leuner, K., Müller, W.E., Kudin, A.P., Kunz, W.S., Zimmermann, A., Roeper, J., Wenzel, D., Jendrach, M., García-Arencíbia, M., Fernández-Ruiz, J., Huber, L., Rohrer, H., Barrera, M., Reichert, A.S., Rüb, U., Chen, A., Nussbaum, R.L., Auburger, G., 2009. Parkinson phenotype in aged PINK1-deficient mice is accompanied by progressive mitochondrial dysfunction in absence of neurodegeneration. PLoS One 4, e5777.

Grünewald, A., Gegg, M.E., Taanman, J.W., King, R.H., Kock, N., Klein, C., Schapira, A.H., 2009. Differential effects of PINK1 nonsense and missense mutations on mitochondrial function and morphology. Exp. Neurol. 219, 266–273.

Haque, M.E., Thomas, K.J., D'Souza, C., Callaghan, S., Kitada, T., Slack, R.S., Fraser, P., Cookson, M.R., Tandon, A., Park, D.S., 2008. Cytoplasmic Pink1 activity protects neurons from dopaminergic neurotoxin MPTP. Proc. Natl. Acad. Sci. U. S. A. 105, 1716–1721.

Hofhaus, G., Johns, D.R., Hurko, O., Attardi, G., Chomyn, A., 1996. Respiration and growth defects in transmitochondrial cell lines carrying the 11778 mutation associated with Leber's hereditary optic neuropathy. J. Biol. Chem. 271, 13155–13161.

Jackson-Lewis, V., Przedborski, S., 2007. Protocol for the MPTP mouse model of Parkinson's disease. Nat. Protoc. 2, 141–151.

Kawajiri, S., Saiki, S., Sato, S., Sato, F., Hatano, T., Eguchi, H., Hattori, N., 2010. PINK1 is recruited to mitochondria with parkin and associates with LC3 in mitophagy. FEBS Lett. 584, 1073–1079.

Kim, Y., Park, J., Kim, S., Song, S., Kwon, S.K., Lee, S.H., Kitada, T., Kim, J.M., Chung, J., 2008. PINK1 controls mitochondrial localization of Parkin through direct phosphorylation. Biochem. Biophys. Res. Commun. 377, 975–980.

King, M.P., Attardi, G., 1989. Human cells lacking mtDNA: repopulation with exogenous mitochondria by complementation. Science 246, 500–503.

Lambert, A.J., Buckingham, J.A., Boysen, H.M., Brand, M.D., 2010. Low complex I content explains the low hydrogen peroxide production rate of heart mitochondria from the long-lived pigeon, Columba livia. Aging Cell 9, 78–91.

Liu, W., Vives-Bauza, C., Acin-Perez, R., Yamamoto, A., Tan, Y., Li, Y., Magrane, J., Stavarache, M.A., Shaffer, S., Chang, S., Kaplitt, M.G., Huang, X.Y., Beal, M.F., Manfredi, G., Li, C., 2009. PINK1 defect causes mitochondrial dysfunction, proteasomal deficit and alpha-synuclein aggregation in cell culture models of Parkinson's disease. PLoS One 4, e4597.

Matsuda, N., Sato, S., Shiba, K., Okatsu, K., Saisho, K., Gautier, C.A., Sou, Y.S., Saiki, S., Kawajiri, S., Sato, F., Kimura, M., Komatsu, M., Hattori, N., Tanaka, K., 2010. PINK1 stabilized by mitochondrial depolarization recruits Parkin to damaged mitochondria and activates latent Parkin for mitophagy. J. Cell Biol. 189, 211–221.

Narendra, D., Tanaka, A., Suen, D.F., Youle, R.J., 2008. Parkin is recruited selectively to impaired mitochondria and promotes their autophagy. J. Cell Biol. 183, 795–803.

Narendra, D.P., Jin, S.M., Tanaka, A., Suen, D.F., Gautier, C.A., Shen, J., Cookson, M.R., Youle, R.J., 2010. PINK1 is selectively stabilized on impaired mitochondria to activate Parkin. PLoS Biol. 8, e1000298.

Park, J., Lee, S.B., Lee, S., Kim, Y., Song, S., Kim, S., Bae, E., Kim, J., Shong, M., Kim, J.M., Chung, J., 2006. Mitochondrial dysfunction in *Drosophila PINK1* mutants is complemented by *parkin*. Nature 441, 1157–1161.

Pridgeon, J.W., Olzmann, J.A., Chin, L.S., Li, L., 2007. PINK1 protects against oxidative stress by phosphorylating mitochondrial chaperone TRAP1. PLoS Biol. 5, e172.

Reitzer, L.J., Wice, B.M., Kennell, D., 1979. Evidence that glutamine, not sugar, is the major energy source for cultured HeLa cells. J. Biol. Chem. 254, 2669–2676.

Reynafarje, B., Costa, L.E., Lehninger, A.L., 1985. O_2 solubility in aqueous media determined by a kinetic method. Anal. Biochem. 145, 406–418.

Sandebring, A., Thomas, K.J., Beilina, A., van der Brug, M., Cleland, M.M., Ahmad, R., Miller, D.W., Zambrano, I., Cowburn, R.F., Behbahani, H., Cedazo-Mínguez, A., Cookson, M.R., 2009. Mitochondrial alterations in PINK1 deficient cells are influenced by calcineurin-dependent dephosphorylation of dynamin-related protein 1. PLoS One 4, e5701.

Trojanowski, J.Q., 2003. Rotenone neurotoxicity: a new window on environmental causes of Parkinson's disease and related brain amyloidoses. Exp. Neurol. 179, 6–8.

Twig, G., Elorza, A., Molina, A.J., Mohamed, H., Wikstrom, J.D., Walzer, G., Stiles, L., Haigh, S.E., Katz, S., Las, G., Alroy, J., Wu, M., Py, B.F., Yuan, J., Deeney, J.T., Corkey, B. E., Shirihai, O.S., 2008. Fission and selective fusion govern mitochondrial segregation and elimination by autophagy. EMBO J. 27, 433–446.

Valente, E.M., Abou-Sleiman, P.M., Caputo, V., Muqit, M.M., Harvey, K., Gispert, S., Ali, Z., Del Turco, D., Bentivoglio, A.R., Healy, D.G., Albanese, A., Nussbaum, R., González-Maldonado, R., Deller, T., Salvi, S., Cortelli, P., Gilks, W.P., Latchman, D.S., Harvey, R.J., Dallapiccola, B., Auburger, G., Wood, N.W., 2004. Hereditary early-onset Parkinson's disease caused by mutations in *PINK1*. Science 304, 1158–1160.

Vives-Bauza, C., Zhou, C., Huang, Y., Cui, M., de Vries, R.L., Kim, J., May, J., Tocilescu, M.A., Liu, W., Ko, H.S., Magrane, J., Moore, D.J., Dawson, V.L., Grailhe, R., Dawson, T.M., Li, C., Tieu, K., Przedborski, S., 2010. PINK1-dependent recruitment of Parkin to mitochondria in mitophagy. Proc. Natl. Acad. Sci. U. S. A. 107, 378–383.

Wood-Kaczmar, A., Gandhi, S., Yao, Z., Abramov, A.Y., Miljan, E.A., Keen, G., Stanyer, L., Hargreaves, I., Klupsch, K., Deas, E., Downward, J., Mansfield, L., Jat, P., Taylor, J., Heales, S., Duchen, M.R., Latchman, D., Tabrizi, S.J., Wood, N.W., 2008. PINK1 is necessary for long term survival and mitochondrial function in human dopaminergic neurons. PLoS One 3, e2455.

Yang, Y., Ouyang, Y., Yang, L., Beal, M.F., McQuibban, A., Vogel, H., Lu, B., 2008. Pink1 regulates mitochondrial dynamics through interaction with the fission/fusion machinery. Proc. Natl. Acad. Sci. U. S. A. 105, 7070–7075.

5. 遺伝的因子，遺伝学的見地からのパーキンソン病 update

—パーキンソン病にどこまで遺伝的要因が関与しているか？—

富山弘幸
Hiroyuki Tomiyama

はじめに

パーキンソン病（PD）はアルツハイマー病に次いで2番目に多い神経変性疾患であり，今後高齢化社会が進むにつれ，ますます患者が増えていくものと考えられるcommon diseaseである．その90～95%は孤発型であるが，約5～10%に家族性PD（FPD）を認め，PDの発症に遺伝的因子が少なからず関与していると考えられる．PDの根本の原因は未だ不明だが，加齢因子とともに遺伝的因子と環境因子の相互作用により発症するという考え方が主流となってきている．ではそれらは実際どの程度PDの発症に関わっているのであろうか．その点を明らかにすることはPDの原因，発症機序を考え，治療法の開発に繋げる上で重要である．

環境因子の一つとして，1980年代にMPTP-induced parkinsonismが報告され，PDの病態にミトコンドリアの関与が明らかにされた[1,2]．一方，遺伝的因子に関し，1997年*α-synuclein*（*PARK1*）がFPDの原因遺伝子として初めて同定され[3]，α-synucleinはPDの病理学的診断マーカーとしてのレビー小体の主要構成成分であることが報告された[4]．次いで*α-synuclein*の重複による遺伝子量の増加に相関して*α-synuclein*が過剰発現し，レビー小体がより形成されやすくなると報告され[5]，*α-synuclein*がレビー小体の形成に大きく関わっていることが示唆された．

*α-synuclein*同定の翌1998年，2番目の原因遺伝子として*parkin*（*PARK2*）が我が国で単離され[6]，ユビキチンリガーゼとしての機能が報告された[7]．そのホモ変異症例はレビー小体をもたないことが報告され[8]，レビー小体の形成，パーキンソニズムの発症機序へのFPDの原因遺伝子の関与についての分子遺伝学的研究が盛んになった．

その後ここ10年，FPD研究の進歩はめざましく，新しい遺伝子座や遺伝子の報告が続いている．これまでに*PARK1～16*までと*NR4A2*が遺伝子座として報告され，常染色体優性遺伝性PD（ADPD）として*α-synuclein*[3]，*UCH-L1*[9]，*LRRK2*[10,11]，常染色体劣性遺伝性PD（ARPD）として*parkin*[6]，*PINK1*[12]，*DJ-1*[13]とそれぞれ3つずつ，計6つの原因遺伝子が報告されている．

一方，原因遺伝子の同定によりその機能解析，動物モデルの研究が進んでいる．神経変性過程におけるARPDの遺伝子産物そのもののミトコンドリアへの関与も明らかにされつつある．FPD関連遺伝子の研究は日進月歩であり，遺伝的因子の知見が孤発性PD（SPD）の発症メカニ

ズムの解明，治療の開発に大きく寄与するものと考えられてきている．

また，*α-synuclein* や *LRRK2* の一塩基多型（SNP）は SPD の risk factor となり感受性遺伝子としても働くことが報告されており，FPD と SPD の発症には共通の機構があると考えられる．さらに最近，常染色体劣性遺伝性疾患の Gaucher 病の原因遺伝子である *GBA* ヘテロ変異が PD の危険因子となることが報告されている[14]．日本人では，現在報告されている *LRRK2* G2385R[15]およびいくつかの *GBA* ヘテロ変異[16]だけでも，実に PD の約 10%に認める頻度の高い危険因子であることがわかっており，発症に関わる遺伝的因子がまだ多数存在している可能性が高い．

このように，PD において，遺伝的因子はこれまで考えられていた以上に大きな発症の原因または背景となっていることが想定されてきている．また，たくさんの遺伝学的知見の蓄積により，FPD におけるレビー小体の有無など多様な臨床像が明らかになり，PD は単一の疾患概念ではなく，あるスペクトラムにのってくる heterogeneous な疾患概念であると考えられてきている．本稿ではこれまでに蓄積された多くのエビデンスを提示し，最新の知見，今後の期待し得る展望も含め review したい．

■A．加齢，環境因子のエビデンス

PD の有病率は 10 万人に 120〜130 人（約 1000 人に 1 人，0.1%）と考えられ，加齢とともに患者数は増加し，55 歳以上の約 1%，65 歳以上の約 2%，75 歳以上の約 3%に PD 患者が存在するともいわれ，加齢は明らかな危険因子となっている[17]．このことは，PD には時間経過に依存した発症機構，進行過程が存在することを示しているのかもしれない．PD は脳内ドパミンが約 80%減少したときに発症するとも考えられているが，加齢と共に何らかの機序で徐々にドパミン神経細胞が脱落し発症していくことが示唆される．PD を発症していない剖検例での incidental Lewy body disease の存在，Lewy body disease のスペクトラムについての考え方もこのことと同様のことなのかもしれない．

環境因子の考え方としては，1980 年代にヘロインの不純物 MPTP（1-methyl-phenyl-1,2,3,6-tetrahydropyridine）による若年発症のパーキンソニズム（MPTP induced parkinsonism），剖検所見での黒質神経細胞脱落の報告があった[1,2]．MPTP induced parkinsonism の報告，研究から，環境因子，ミトコンドリア機能異常が PD の病態に関与することが明らかにされた．MPTP とパーキンソニズムの関連は明らかであり，MPTP は実験モデルにもよく使われてきている．一時期は同じような神経毒性の高い物質などが盛んに調べられたが，少なくとも暴露の危険の高いものでは，明らかな危険因子はみつかっていない．

MPTP は特殊な物質である一方，より一般的な環境因子では，危険因子として頭部外傷歴，金属暴露，農薬暴露，井戸水などがあげられている．しかしながら，これらはそれ程頻度が高くないと考えられ，少なくとも PD 発症の主な危険因子であることは考えにくい．

保護的因子としてはカフェイン，喫煙が報告され，これらは世界中で日常ありふれた因子であるが，今のところ強い保護因子ではないと考えられている．環境因子については暴露歴，暴露基準の評価が難しく，現時点でどれもどこまで PD に関与しているのか，未だエビデンスには乏し

い状況である．

■B．遺伝的因子のエビデンス

環境因子と遺伝的因子の関与を考える上で大切な知見として，一卵性双生児での研究がある．PET（positron emission tomography）での異常所見とも合わせると，一卵性双生児間では疾患一致率は100％ではないものの，二卵性双生児の疾患一致率に比べ約3倍以上高いと報告された[18]．これは同じ遺伝情報で発症が100％は規定されないが，関与がより強いことを示唆する．またアイスランドにおける全国民を対象とした遺伝子解析疫学調査により，50歳以上のPD患者の配偶者の発症率に比べ同胞，子供など血縁者の発症危険率は有意に高く，PDの発症には遺伝的因子が関わっていることが示唆された．

一方，Roccaらの近年の疫学調査報告により，66歳をカットオフとしてそれより若い場合を若年性PDとする概念が生まれてきている．この報告によれば，66歳以下で発症する場合，家系内発症の相対危険度は2倍にのぼると報告されている．

また，家族内発症例についての欧州での疫学調査では，一親等内の発病が，患者で10.3％，controlでは3.5％（オッズ比3.2，95％CI 1.6-6.6）と報告され，明らかな家族内集積の傾向が示されている[19]．

このように，遺伝的因子を背景に，環境因子との相互作用のもとPDが発症することが示唆されるとともに，遺伝子の関与がかなり強いものと考えられてきている．

ではどこまで遺伝的因子がPDの発症に関与しているのであろうか？

単一遺伝子異常によるPDの存在から，遺伝的因子の関与が確立したものになった訳であるが，この命題に答を与えてくれるのはFPDの研究であり，以下，ここでは遺伝学的見地からFPD関連の遺伝子について中心に述べたい．

■C．家族性パーキンソン病，*PARK*シリーズの分類

現在までに*PARK1*～*16*までと*NR4A2*が遺伝子座（染色体での同定された存在部位）として報告され，FPDの原因遺伝子として6つが同定されている（表1）．*Nurr1*[20]は*NR4A2*の原因遺伝子として報告されたが，その意義は十分確立されていない．最近も新しい遺伝子座や遺伝子の同定が続いており，つい最近*PARK16*が報告された[21,22]．*PARK*シリーズの遺伝子のうち非典型的パーキンソニズムの原因遺伝子として，*ATP13A2*[23]，*PLA2G6*[24]，*FBXO7*[25]などが報告され，その他FPDの原因遺伝子としての意義が十分確立していないものとして，*GIGYF2*[26]，*Omi/HtrA2*[27]なども報告されている．

1．常染色体優性遺伝性パーキンソン病（ADPD）

a．*SNCA*，α-*synuclein*（*PARK1*，*PARK4*）

1990年に臨床症候が報告された大きなADPDの家系，Contursi家系から，1997年にFPDの原因遺伝子変異として初めてα-*synuclein* A53T変異が同定された[3]．これまでにA53Tに加え，

表1　家族性パーキンソン病，*PARK* シリーズの分類

遺伝子シンボル	遺伝子座	遺伝形式	遺伝子	レビー小体
PARK1, 4 (SNCA)	4q21	AD	*α-synuclein*	+
PARK2	6q25.2-q27	AR	*parkin*	−（+ *1, *2）
PARK3	2p13	AD	?	+
PARK5	4p14	AD	*UCH-L1*	?
PARK6	1p35-p36	AR	*PINK1*	?（+ *2）
PARK7	1p36	AR	*DJ-1*	?
PARK8	12q12	AD	*LRRK2*	+/−
PARK9	1p36	AR	*ATP13A2*	?
PARK10	1p32	SP（感受性遺伝子）	?	?
PARK11	2q36-q37	AD	*GIGYF2*	?
PARK12	Xq21-q25	SP（感受性遺伝子）	?	?
PARK13	2p12	AD	*HtrA2/Omi*	?
PARK14	22q13.1	AR	*PLA2G6*	?
PARK15	22q12-q13	AR	*FBXO7*	?
PARK16	1q32	SP	?	?
GBA	1q21	SP	*glucocerebrosidase*	+
SCA2	12q24	AD	*ataxin-2*	+
NR4A2	2q22-q23	AD	*Nurr1*	?

AD：autosomal dominant，AR：autosomal recessive，SP：sporadic
*1：+；ホモ変異で1例，複合ヘテロ変異で2例報告．　*2：+；ヘテロ変異で報告あり

A30P[28]，E46K[29]の3つのミスセンス変異が報告されているが，変異の頻度はごく稀とされている．臨床像はやや若年発症のパーキンソニズムに加え，一部に dementia を認める．A53T 変異はその後 11 家系の報告があり，ギリシャ起源の家系にほぼ限られ，全て共通の祖先による創始者効果が示唆されている．最近韓国人からも報告があり[30]，別の祖先であることが示唆された．A53T 変異症例は SPD によく似ているが，平均発症年齢は 45.6 歳で認知症の合併が多い．一方 A30P 変異はドイツの家系より見つかり，平均発症年齢は 54.3 歳で初期症状としても認知症を伴うことが多い可能性が報告された．A30P 変異症例の病理像も黒質，青斑核，迷走神経背側核などをはじめ広範に α-synuclein の沈着を認め，一般の SPD と比べより強い変化を認めていた[31]．E46K 変異はスペインの家系で報告され，発症年齢は 50〜65 歳で認知症は伴うことが多く，病理像でび漫性レビー小体病であることが確認されている．

これらの変異による機能解析では，変異体があることにより α-synuclein がオリゴマーを形成し，凝集，蓄積しやすくなることが考えられている．A30P の変異により α-synuclein と脂質との結合が低下し[32]，A53T の変異により膜の流動性が変化することも報告されている[33]．A53T，A30P，E46K の3つの変異全てが脂質結合部位にあるのは，α-synuclein と脂質との結合が，膜安定化，立体構造の変化による毒性を抑えることを示唆しているのかもしれない．

α-synuclein 変異患者の病理所見では脳幹にレビー小体を認めている．α-synuclein は PD の病理学的診断の指標とされてきたレビー小体の主要構成成分であり，さらには多系統萎縮症の glial

cytoplasmic inclusion（GCI）の構成成分でもあると報告されたことから，FPD のみならず SPD におけるレビー小体形成，さらにはより広く異常蛋白の凝集・蓄積機序，神経細胞変性機序の解明に重要な意義をもつと考えられている．*α-synuclein* 変異は gain of toxic function をきたし，神経変性に関わると考えられている．PD をはじめとした *α-synuclein* の蓄積による synucleinopathy という疾患群の概念も広がり，アルツハイマー病をはじめとした tau の蓄積による tauopathy と synucleinopathy という 2 つの概念が少なからずオーバーラップすることも指摘されてきており，TDP-43 proteinopathy[34,35] も含め代表的な変性疾患群の神経変性過程において共通の機構が存在する可能性も考えられている．α-synuclein の分解系においては，リソゾーム系が注目されているが[36]，α-synuclein の過剰発現は神経変性過程で重要な ubiquitin-proteasome system（UPS）を抑制することも報告されている．α-synuclein や tau（や TDP-43）などの分子が過剰産生あるいは異常蓄積する機序を解明することが神経変性疾患を克服するカギになるとも考えられている．

2003 年に，*PARK4* として 4 番染色体短腕にマップされていたアイオワ家系は *α-synuclein* 遺伝子の 3 重複 triplication である（*PARK4* は実は *PARK1* と同じ遺伝子座にあり，原因遺伝子は同じ *α-synuclein* だった）ことが判明した[5]．*α-synuclein* 変異には duplication（2 重複）の報告もあり，日本でも複数の家系でみつかっており，*α-synuclein* multiplication は ADPD の 2%くらいを占め従来の欧米からの報告ほど稀ではない可能性がある[37]．遺伝子重複による *α-synuclein* の過剰発現が病態に関与していることが示唆されており，*α-synuclein* triplication 例は duplication や孤発型 PD に比し，発症年齢の若年化および dementia の合併など症状の重症化（gene dose effect）が報告され，triplication 例の病理像はび漫性レビー小体病である[5]．当初 duplication 症例では認知症を合併しないと報告されていたが，我々の経験した duplication 症例では認知症を合併しており，その病理像ではレビー小体とともに，GCI を認めたことは大変興味深い[37,38]．また，*α-synuclein* 2 重複変異で浸透率が 33%（2/6）と低い家系が存在しており，平均発症年齢を遥かに超えても発症していない未発症キャリアが存在することがあり[37]，その発症者との違いがわかれば *α-synuclein* が PD の発症機序にどのような役割をもつかということの知見が得られるのかもしれない．さらに最近，大規模解析により *α-synuclein* の SNP が MSA の危険因子になることも報告された[39]．*α-synuclein* の発現をコントロールすることが，PD のみならず MSA も含む synucleinopathy の治療のターゲットになる可能性がある．*α-synuclein* multiplication は FPD の約 1～2%未満と報告されているが，SPD でも存在することが報告されており，孤発例における意義も認識されてきている[40]．

一方，*α-synuclein* の遺伝子調節領域の変化も発現を増加させることで発症に関わる可能性が考えられ，*α-synuclein* のプロモーター領域に近い多型 NACP-Rep1 が SPD の危険因子になると報告された[41]．本邦においても SNP 解析が行われ，intron 4 に存在する SNP が感受性遺伝子として同定された[42]．この SNP を持つとやはり発現レベルが増加することが証明されている[42]．野生型の遺伝子重複も含めて *α-synuclein* の過剰発現が PD，synucleinopathy の発症機序を考える上で重要であると考えられている．

b. *LRRK2, leucin rich repeat kinase 2*（*PARK8*）

PARK8 は 1978 年に報告された ADPD の大家系である相模原家系[43]より 2002 年に遺伝子座が決められ[44]，欧米の家系から 2004 年に *LRRK2* が同定された[10,11]．*α-synuclein* と比べ変異の頻度はかなり高く，ADPD の 5〜10%前後，孤発例の 1〜2%前後に及ぶと報告されており[45-47]，特に FPD の原因遺伝子の中でも FPD のみならず SPD における関与も大きいと注目されている[47]．これまでに約 20 個の原因を疑う遺伝子変異が報告されているが，なかでも G2019S 変異はアラブ系やユダヤ系人種および白人に多く，実に北アフリカアラブ人の PD の 30〜41%を占め[48]，次いで南欧に多くハプロタイプ解析により約 2250 年前からの創始者効果が示唆されている[49]．G2019S 変異はアジアでは稀で本邦では 3 家系の報告があるが，上記人種と同じ創始者効果は否定的である[50,51]．一方，トルコ人でも G2019S 変異が同定され，日本人のハプロタイプと同じであり，共通の祖先と考えられ，民族移動の歴史を示唆し大変興味深い[52]．相模原家系は G2019S 変異の隣にあるアミノ酸の I2020T 変異をもち[53]，本邦で相模原家系以外にも 2 家系が報告されている[50]．こちらの変異については日本人では同じハプロタイプを示しており，相模原家系と同じ先祖から分かれた家系と推定される[50]．一方，病的変異とは別に台湾で G2385R[54]や R1628P[55]という変異が報告され，SPD の危険因子として，発症に関与する結果が得られたことはさらに興味深い．G2385R については 4800 年くらい前のアジア人で生じた創始者効果と推定されている[56]．

PD は今から約 200 年前の 1817 年に，James Parkinson が“An Essay on the Shaking Palsy”で初めて報告した疾患であるが，FPD の原因遺伝子である *LRRK2* の遺伝学的研究により，そのルーツは推定 2250 年くらい前にまでさかのぼることができている[49]．人類のルーツは北アフリカにあり，そこから大昔にヨーロッパ，中東をはじめ周囲に移動していったと考えられているが，人類発生と民族大移動の歴史も，PD の発生と移動の歴史も一致している可能性が示唆され，人類遺伝学的に大変興味深い．

LRRK2 変異症例の臨床像は，基本的には片側発症が多く，レボドパの反応性がよいパーキンソニズムで，一般の SPD と区別が困難であるが，変異や症例によって多様な臨床像や病理像をとり得ることは最も興味深い点である．発症年齢は 20 歳代の early-onset PD もあり広範囲に及ぶが[57,58]，50〜60 代以降の late-onset PD が多い[59]．MIBG 心筋シンチは正常例と低下例とがある[50]．G2019S 変異では SPD と同様，F^{18}-dopa PET で F^{18}-dopa の取り込み低下がみられた．睡眠障害は 85%に認めたという報告があるが，嗅覚障害は *parkin* 変異症例と同様に比較的稀とされる[60,61]．LRRK2 はレビー小体の構成成分であると報告される一方[62]，レビー小体がないものからび漫性レビー小体病までレビー小体の出現は変異によってもさまざまで，進行性核上性麻痺や筋萎縮性側索硬化症等の病理報告もある[63]．さらに相模原家系ではレビー小体が存在しない症例と，GCI を認めた線条体黒質変性症（多系統萎縮症，MSA）の症例も報告されており[53]，同一家系，同一変異でも多様な病理像をとりうることは神経変性機序を考える意味でも興味深い[11]．

蛋白の機能は今のところ不明であるが，LRRK2 は ubiquitous に発現しており，α-synuclein と tau 等の上流に位置しそれらのリン酸化に関与する多機能蛋白として，多様な病理像と関連して